Processes Governing Primary Biofilm Formation

JAMES D. BRYERS, *Swiss Federal Institute for Water Resources and Water Pollution Control (EAWAG), Dübendorf CH-8600, Switzerland,* and WILLIAM G. CHARACKLIS, *College of Engineering, Montana State University, Bozeman, Montana 59717*

Summary

Biofilm accumulation under turbulent flow conditions on the surface of a circular tube is the net result of several processes including the following: 1) transport and firm adhesion of soluble components and microbial cells to the surface; 2) metabolic conversions within the biofilm including growth and maintenance decay processes; 3) detachment of portions of the biofilm and reentrainment in the bulk fluid. Experiments in a tubular reactor were designed to measure the rates of these processes during the early stages of biofilm accumulation as a function of the Reynolds number and suspended biomass concentration. Results indicate deposition (i.e., combined transport and adsorption) is only important in the very early stages of biofilm accumulation and is significantly influenced by suspended biomass concentration but not Reynolds number. Biofilm decay rates are negligible for the thin biofilms encountered in these experiments. Net biofilm production rates in all experiments decrease to the same level and this level is not affected by changes in Reynolds number or suspended biomass concentration. Biofilm detachment rate increases continuously with biofilm accumulation and with increasing Reynolds number.

INTRODUCTION

Apparently, the majority of microbial activity in natural waters occurs at solid-liquid or air-liquid interfaces.[1-3] Microbial films can play a beneficial role in certain wastewater treatment operations (e.g., rotating biological contactors and trickling bed filters), natural stream purification, and specific fermentation processes (e.g., vinegar production from ethanol). However, biofilms, mostly bacterial, also form in heat exchangers, water transport lines, and secondary oil recovery systems creating increased frictional resistance,[4-6] accelerated corrosion,[7,8] and reduced heat transfer efficiency.[9,10]

Individual Processes Contributing to Biofilm Accumulation

Biofilms develop in a sigmoidal fashion (Fig. 1). Evidence suggests that biofilm development is the net result of the following transport and biological reaction rate processes:

Biotechnology and Bioengineering, Vol. XXIV, Pp. 2451-2476 (1982)
 CCC 0006-3592/82/112451-26$03.60

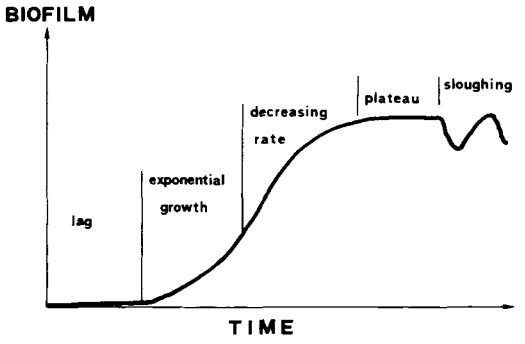

Fig. 1. Biofilm development.

1) Adsorption of dissolved organics at the wetted surface. Investigations report that materials of diverse surface properties are conditioned by an adsorbed organic layer within minutes of exposure to natural water.[11-14]

2) Transport of microbial particles to the surface. Particles suspended in a turbulent flow stream can be transported to the surface by either molecular diffusion, turbulent eddy transport, sedimentation, and thermophoresis.[15-17]

3) Microorganism adhesion to the surface. Research suggests that bacterial cell adhesion to a solid is a two-stage process: reversible adhesion followed by irreversible adhesion. Adhesion studies have generally been conducted at very low fluid shear rates.[18-22] Biofilm accumulation rates in these studies may have been mass-transfer rate limited and, therefore, the data are not necessarily applicable to turbulent flow conditions.

4) Biofilm production. Biofilm production is the net accumulation of attached material due to cellular reproduction and microbial production of extracellular polymers.

5) Biofilm detachment. During biofilm development, portions of biofilm peel away from the surface and are entrained in the fluid flow. Detachment is a process of continuous biofilm removal and is highly dependent on hydrodynamic conditions.[23,24] "Sloughing," however, appears to be a random, massive removal of biofilm attributed to oxygen/nutrient limitations deep within the biofilm.

In summary, biofilm formation is the net result of several processes occurring simultaneously (Fig. 2). Naturally, certain processes can predominate over others at specific times during biofilm development.

Past research on biofilm development in turbulent flow systems has focused on metabolic processes within established or mature biofilms and on biofilm detachment.[23,25] However, this article deals with the various physical and metabolic processes contributing to "primary" biofilm accumulation. Primary biofilms are defined here as biofilm accumulation prior to significant increases in fluid frictional resistance. Consequently, results reported here are restricted to very thin (biofilm thickness $\leq 80\mu m$) aerobic biofilms. Specific objectives of the study were the following: 1) to develop a biofilm

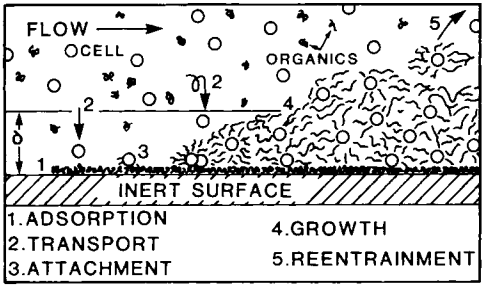

Fig. 2. Processes contributing to biofilm accumulation; δ represents the viscous sublayer thickness. No scale is intended.

detection method sensitive to the early stages of biofilm formation; 2) to derive a kinetic expression for net biofilm accumulation rate as a function of microbial activity and hydrodynamic parameters; 3) to analyze the fundamental processes influencing accumulation in the early stages of biofilm formation.

Results pertaining to the first two objectives are presented elsewhere.[24,26,27] This article presents results dealing with the process dynamics of primary fouling biofilm development, i.e., the early stages of biofilm development.

EXPERIMENTAL

Reactor System

Two completely stirred tank reactors (CSTR), in series, were used in this study (Fig. 3) so that operation of the first CSTR was independent of the operation of the second CSTR. The first reactor was a conventional chemostat (CSTR 1). The second reactor (CSTR 2) was a tubular reactor with internal recycle flow. Recycle flow rate in CSTR 2 was always much greater than the volumetric flow rate of CSTR 2 influent. Two separate substrate feed systems delivered concentrated substrate solutions and dilution water to each reactor. The substrate was a mixture of glucose and trypticase soy broth (TSB). Residence times in CSTRs 1 and 2 were maintained at 3 and 0.25 h, respectively. CSTR 1 served only as a source of suspended biomass for CSTR 2. A fraction of the CSTR 1 effluent was diverted to CSTR 2 where it was mixed with dilution water and fresh substrate. Biofilm development under turbulent flow conditions was observed in CSTR 2. Experiments in CSTR 2 were conducted for elapsed times of 70 h before the reactor was cleaned and reassembled. There was no interruption of the suspended biomass growth in CSTR 1 throughout the experimentation period (44 days). Details of the reactor system can be found elsewhere.[24] Table I summarizes the pertinent operating characteristics of both reactors.

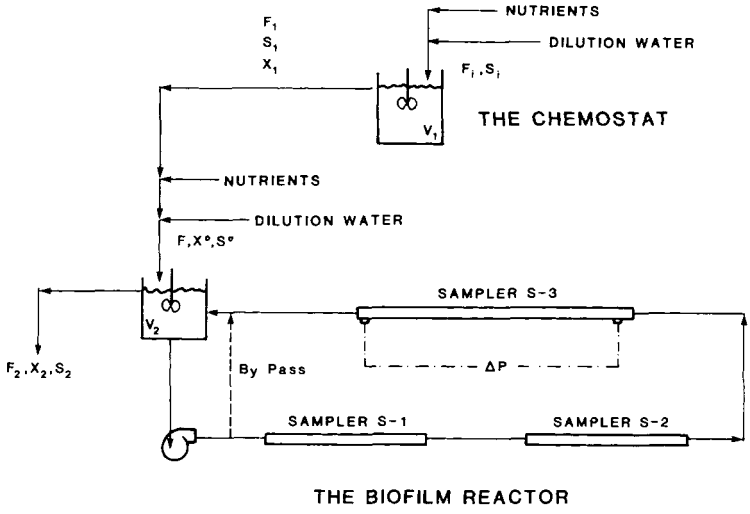

Fig. 3. Reactor system details.

Two types of tubular test sections were employed in CSTR 2. Details of the test sections, termed S-1, S-2, and S-3, are shown in Figures 4 and 5. Test sections S-1 and S-2 were identical in design and each consisted of twenty 1.27 cm i.d. × 5.2-cm-long cylindrical Pyrex sample tubes within a stainless-steel outer sleeve. Sample tubes were periodically withdrawn to chemically determine biofilm accumulation. Test section S-3 was a 1.27 cm i.d. × 91.4-cm-long Pyrex glass tube with pressure taps 2.5 cm from each end. Pressure drop across this section was measured with an inclined mercury manometer (range was 0-15.2 cm Hg). Biofilm development on the inner surface of S-3 was also observed with an optical microscope (total magnification of 100×).

Analytical

Glucose concentrations in stock solutions only were determined using the Glucostat (Worthington Biochemical) procedure.

Chemical oxygen demand (COD) was used to indirectly measure the amount of organic carbon in the bulk fluid of both reactors and in the biofilm attached to sample tubes from units S-1 and S-2. The *Standard Methods* COD procedure[28] was modified by diluting the dichromate and ferrous ammonium sulfate reagents by ten to detect anticipated low levels of oxidizable carbon present.

Effluent suspended biomass concentration was determined by filtration and gravimetric measurement. Periodically, two 100-mL effluent samples were filtered though tared 0.45-μm Nucleopore filters. Filters were dried at 60°C for three hours and stored in a dessicator until weighed.

Biofilm sampling and chemical analysis was performed in the following

TABLE I
Pertinent Characteristics of CSTR 1 and CSTR 2

	CSTR 1: the chemostat	CSTR 2: the biofilm reactor
System specifics		
Reaction volume (cm^3)	3000	4750
Total wetted surface area (cm^2)	1070	5934
Surface area: volume (cm^{-1})	0.36	1.25
Dilution rate (h^{-1})	0.33	4.0
Mean residence time (h)	3.0	0.25
Dilution water flow (cm^3/h)	998	18000
Effluent flow rate (cm^3/h)	1000	19000
Growth specifics		
Inlet substrate TSB: glucose (w/w)	9:1	1:1
Combined concentration		
(mg L^{-1})	1000	20.0
(mg COD L^{-1})	850	28.0
Microbial feed	initial inoculation with heterogeneous population	CSTR 1 effluent
Temperature (°C)	31	31
pH	8.1	7.3
Recycle loop specifics (CSTR 2 only)		
Recycle loop tube length (cm)		1219.0
Inside tube diameter (cm)		1.27
Recycle Reynolds number	13000	26000
Recycle flow rate (cm^3/s)	104	208
Recycle velocity (cm/s)	82	164
Test sections	S1	S2,3
Length (cm)	91.4	104
Inside diameter (cm)	1.27	1.27
Sample tubes (S2,3)		
Number		40
Length/tube (cm)		5.2
Inner surface area/tube (cm^2)		20.7
Total sampling surface area (cm^2)		830.0
Percent sampling area of total system area		14.0

manner. Biofilm on sample tubes from S-1 and S-2 was determined using the COD analysis. A five-step sample preparation was used to maximize recovery: 1) Sample tubes were removed at prescribed intervals and gently rinsed with distilled water to remove any loosely attached material. 2) The sample tube was placed in 25 mL of double distilled water in a precleaned 2.3 cm i.d. × 20.0-cm-long glass culture tube. 3) The culture tube received one minute of ultrasonic sound to disrupt and disperse all adherent material. 4) Five milli-

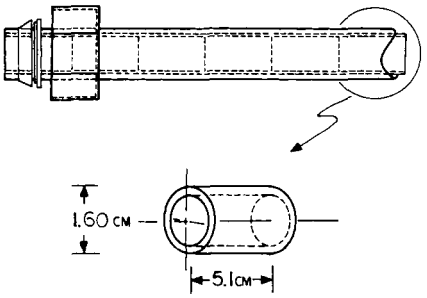

Fig. 4. Details of biofilm test sections, S1 and S2.

liters of concentrated sulfuric acid was then added to the culture tube. 5) Contents of the culture tube, including the acidified biomass suspension and sample tube, were transferred to a precleaned distillation flask for COD analysis.

Biofilm decay measurements. Maintenance requirements cause a decrease with time in biofilm COD during the absence of substrate. This decay rate was determined by measuring the dissolved oxygen (DO) uptake rate of a fouled sample tube. Five fouled sample tubes were removed during latter stages of the experiments from CSTR 2 and were immediately immersed in 50 mL of filtered (0.45-μm) CSTR 2 effluent so that no gas phase existed in the container. All samples were stirred to eliminate mass-transfer limitations. Samples were sacrificed every 30 min to determine the DO content of the fluid. Two additional 50-mL effluent samples served as controls to estimate the DO depletion of the fluid alone over the two hour period. Dissolved oxygen was determined using the azide-modified Winkler method.[28]

RESULTS

The Chemostat: CSTR 1

CSTR 1 was operated continuously for the 44 days of experimentation. Dilution rate was maintained at 0.33 h^{-1} with inlet soluble COD concentration varying from 640 to 850 mg COD/L. Resultant CSTR 1 effluent had total unfiltered COD concentrations ranging from 390 to 400 mg COD/L and

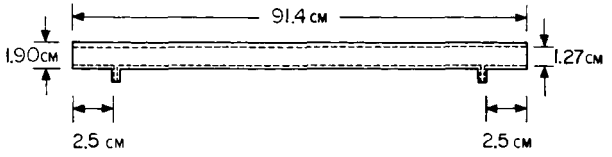

Fig. 5. Details of biofilm test section, S3.

soluble COD concentrations of 40-50 mg COD/L *prior to* dilution. The heterogeneous culture used to inoculate CSTR 1 resulted in a relatively stable population dominated by three organisms: *Klebsiella oxytora, Klebsiella pneumoniae,* and *Enterobacter cloace.* Under these experimental conditions, the mixed culture dilution rate at "washout" and biomass yield are, respectively, 2.2 h^{-1} and 0.42 g biomass/g COD removed.

The Biofilm Reactor: CSTR 2

Operating conditions

Operating conditions for the four experiments carried out in CSTR 2 are given in Table II. Inlet flow to CSTR 2 consisted of dilution water, fresh sterile substrate, and CSTR 1 effluent. Effluent soluble COD from CSTR 1 was approximately 1.5-3.0 mg COD/L *after* dilution and contributed no significant biodegradable carbon to CSTR 2.[24] Primary substrate fed to CSTR 2 in all experiments consisted of 10 mg/L TSB and 10 mg/L glucose after dilution.

Material balances

Presentation of CSTR 2 results is facilitated by material balances for substrate and suspended biomass as well as a constitutive equation for biofilm accumulation:

Substrate:

$$V dS/dt = F(S_i - S) - \mu VX/Y - R_g A/Y \quad (1)$$

TABLE II
Operating Conditions of CSTR 2, the Biofilm Reactor

	Experiment No.			
	1	2	3	4
CSTR 1 effluent suspended biomass concentration (mg COD L^{-1})	370	359	368	380
CSTR 1 effluent delivered to CSTR 2 (cm^3/h)	1000	1000	1000	200
Measured fresh[a] inlet substrate concentration (mg COD L^{-1})	22.7	22.9	33.0	23.8
Measured inlet suspended biomass concentration (mg TSS L^{-1})	19.5	18.9	19.4	4.0
(mg COD L^{-1})	22.2	21.6	22.1	4.6
Reynolds number	13000	13000	26000	13000
Mean residence time (h)	0.25	0.25	0.25	0.25

[a]Fresh substrate delivered to CSTR 2 consisted of 10 mg L^{-1} TSB and 10 mg L^{-1} glucose. Reported concentration is after dilution with CSTR 1 effluent and fresh dilution water.

Suspended Biomass:

$$V\,dX/dt = F(X_i - X) + \mu XV + R_r A - R_d A \tag{2}$$

Attached Biomass:

$$dB/dt = R_g + R_d - R_r \tag{3}$$

where S is the substrate concentration measured as COD ($M\ L^{-3}$); X is the suspended biomass concentration measured as COD ($M\ L^{-3}$); B is the attached biomass measured as COD ($M\ L^{-2}$); t is the time (t); S_i is the inlet substrate concentration measured as COD ($M\ L^{-3}$); X_i is the inlet suspended biomass concentration measured as COD ($M\ L^{-3}$); V is the reactor volume (L^3); A is the reactor surface area (L^2); F is the volumetric flow rate ($L^3\ t^{-1}$); μ is the specific growth rate of suspended biomass (t^{-1}); Y is the biomass yield measured as COD (MM^{-1}); R_g is net biofilm production rate due to metabolic processes measured as COD ($M\ L^{-2}\ t^{-1}$); R_d is the deposition rate of suspended biomass measured as COD ($M\ L^{-2}\ t^{-1}$); R_r is the detachment rate of biofilm measured as COD ($M\ L^{-2}\ t^{-1}$).

These material balances can be simplified with these four assumptions: 1) Rates of accumulation of S and X are assumed at steady state, i.e., $dS/dt = 0$ and $dX/dt = 0$. 2) Although an increase in suspended cell *numbers* is unlikely at residence times of 0.25 h, increases in suspended biomass concentration may be significant. Consequently, suspended biomass growth in CSTR 2 is not ignored. 3) Substrate depletion rate by suspended biomass is also considered significant in CSTR 2 (see assumption 2). 4) Biofilm net growth rate is assumed the sum of biofilm production processes (i.e., growth of organisms and product formation) and biofilm decay requirements, i.e.,

$$R_g = (\mu_p - k_e)B \tag{4}$$

where μ_p is the specific biofilm production rate (t^{-1}) and k_e is the biofilm decay rate (t^{-1}). Equation (4) tacitly assumes specific biofilm production and decay rates are first order in biofilm COD. Equations (1)-(3) now reduce to the following:

$$F(S_i - S) = (\mu_p BA + \mu XV)/Y \tag{5}$$

$$F(X_i - X) = R_d A - \mu XV - R_r A \tag{6}$$

$$dB/dt = (\mu_p - k_e)B + R_d - R_r \tag{7}$$

Figure 6(a) illustrates the progression of CSTR 2 effluent-soluble COD during experiment No. 3. Figure 6(b) illustrates that substrate accumulation ($V\,dS/dt$) is negligible compared to the substrate removal rate, $F(S_i - S)$. Figure 7(a) shows the progression of reactor effluent suspended biomass concentration during experiment No. 3. Figure 7(b) shows that suspended biomass accumulation ($V\,dX/dt$) is negligible compared to the net input of suspended biomass $F(X_i - X)$. Figures 6(b) and 7(b) confirm that dS/dt and

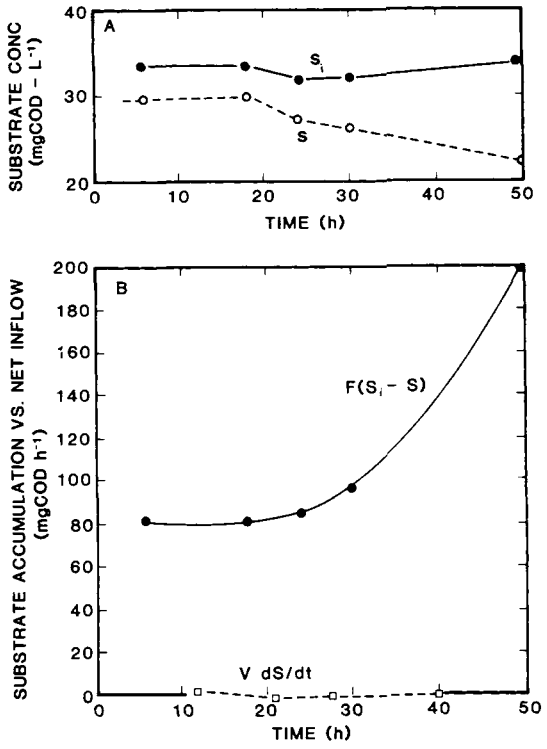

Fig. 6 (A) Influent and effluent soluble COD from CSTR 2 during experiment No. 3. (B) Comparison of substrate accumulation rate (□) to net substrate inflow (●) during experiment No. 3.

dX/dt are nearly zero and, despite some changes in S and X with time, the system can be analyzed as a quasi-steady-state process.

Determining process rates: Equation (7) describes biofilm accumulation throughout an experiment as the sum of four processes: biofilm production ($\mu_p B$), biofilm decay ($k_e B$), suspended biomass deposition (R_d), and biofilm removal (R_r). However, analytical methods provide for direct measurement of only biofilm net accumulation (e.g., B and dB/dt) and the decay rate, $k_e B$.

Consequently, brief changes are periodically made in CSTR 2 experimental conditions to simplify eq. (7). These perturbations consist of depriving CSTR 2 of inlet substrate and/or inlet suspended biomass during four 2-h periods in each experiment. Figure 8 details these perturbations and their intended purpose. This technique allows estimation of the following: 1) Suspended biomass deposition rate (R_d) on the "clean" surface at time equal zero. In further calculations, R_d is assumed constant and independent of biofilm accumulation. 2) Once values of k_e, R_d, and the slope of the bio-

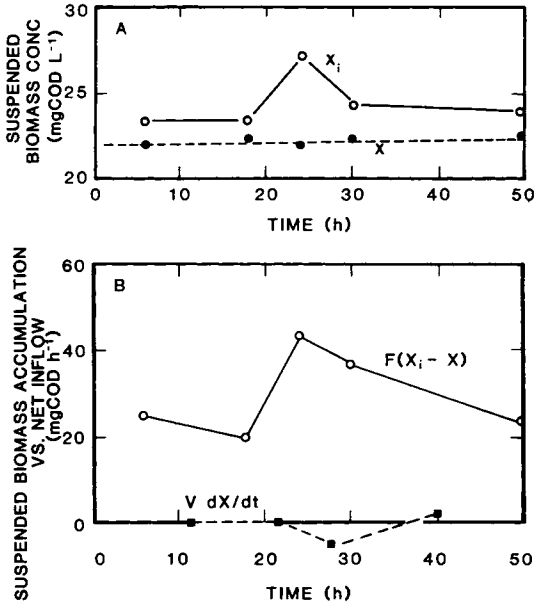

Fig. 7. (A) Influent and effluent biomass from CSTR 2 during experiment No. 3. (B) Comparison of biomass accumulation rate (■) to net biomass inflow (○) during experiment No. 3.

film accumulation curve (i.e., dB/dt) are known, eqs. (9) and (10) can be used to calculate the biofilm removal rate, R_r, at each perturbation period.

Figures 9-12 indicate biofilm COD accumulation for experiment Nos. 1-4, including perturbed and unperturbed intervals. Figure 13 illustrates the linear response in biofilm COD accumulation during four perturbations in experiment No. 2. Biofilm COD accumulation, dB/dt, during these perturbations are presented, for all four experiments, in Table III, along with biofilm decay rate, k_e.

Calculations of R_r in periods 1-4, from data in Table III and eqs. (9) and (10), are summarized in Table IV. Figure 14 illustrates resultant R_r values versus the average biofilm COD present during the perturbation. Data from Trulear and Characklis,[23] obtained from an annular rotating reactor, are also included and indicate a similar magnitude of biofilm removal rates.

Specific biofilm production rates, μ_p, throughout the unperturbed portion of each experiment, are determined using eq. (7) and the appropriate R_d, k_e, and R_r. Figure 15 shows μ_p values as a function of biofilm COD for experiment Nos. 1-4.

DISCUSSION

Deposition

Rate of deposition, R_d, is considered constant throughout any experiment at the value of dB/dt determined during period 1 [refer to eq. (8) and Fig.

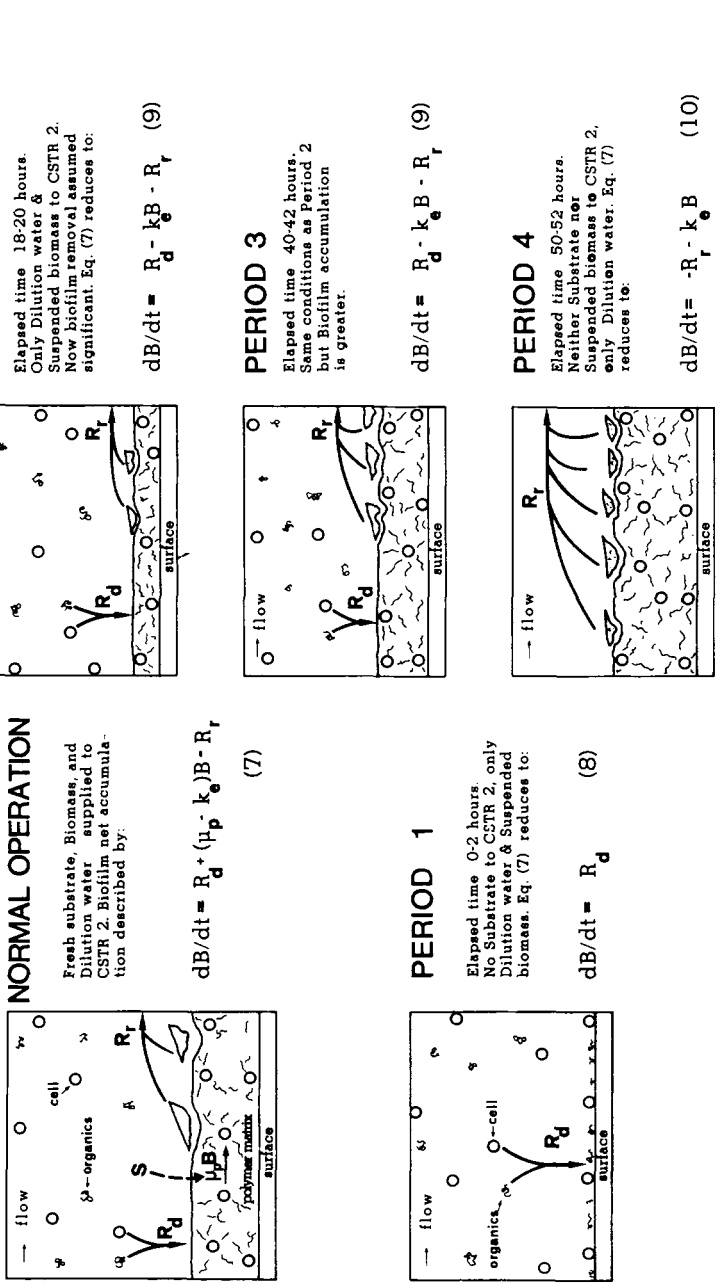

Fig. 8. Description and significance of perturbations to CSTR 2 operating conditions.

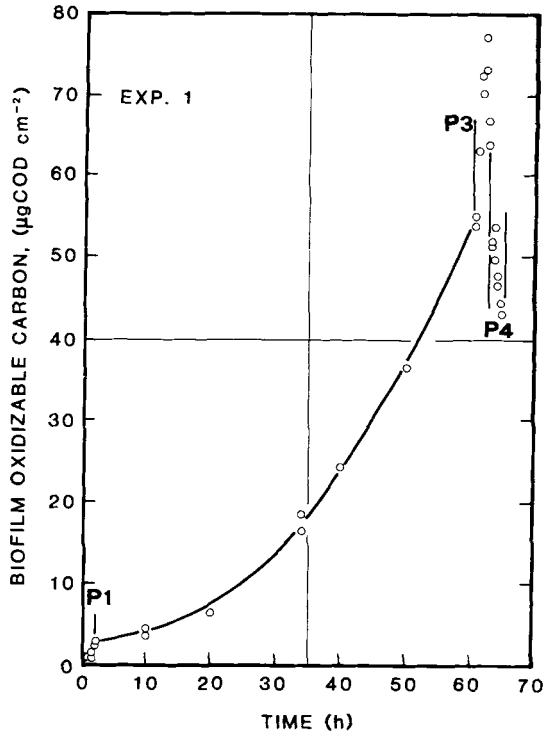

Fig. 9. Biofilm COD accumulation during experiment No. 1, where Re = 1.3×10^4 and X = 19.5 mg/L.

8]. This assumption provides an estimate of deposition rate at "clean" surface conditions and most likely underestimates the enhanced effect a fouled surface would have on particle deposition at later stages of biofilm development.

Adsorption of organic molecules (e.g., polysaccharides and/or glycoproteins) can contribute to the total amount deposited (and rate of deposition) as detected by COD analysis. However, molecular organic adsorption occurs within minutes of exposure[11,12] and the maximum amount of adherent material due to organic adsorption is estimated less than 0.01 μg COD/cm^2.[24] Consequently, rates of organic adsorption are assumed instantaneous and independent of both Reynolds number and suspended biomass concentration.

Mass transfer of particulates across a boundary layer in a turbulent stream can be described by eq. (11):

$$N_x = k_m (X - X_w) \tag{11}$$

where N_x is the net flux of particles to the surface ($M\ L^{-2}\ t^{-1}$); X is the concentration of particles in bulk fluid ($M\ L^{-3}$); X_w is the concentration of par-

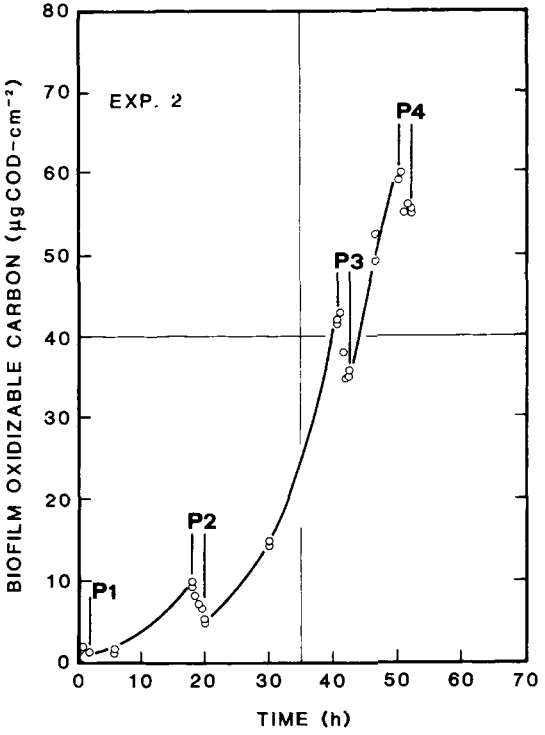

Fig. 10. Biofilm COD accumulation during experiment No. 2, where Re = 1.3×10^4 and X = 18.9 mg/L.

ticles at the fluid-surface interface ($M\ L^{-3}$); and k_m is the mass transfer coefficient ($L\ t^{-1}$). Typically, X_w is presumed zero,[15,16,29] therefore,

$$N_x = k_m X \tag{12}$$

Equation (12) clearly indicates that a change in bulk particle concentration would result in a directly proportional change in particle transport rate. A reduction in suspended biomass concentration from 19.5 to 4.0 mg TSS/L (experiment Nos. 1 and 4, respectively) results in a decrease of 1.2 to 0.3 μg COD $cm^{-2}\ h^{-1}$ in measured deposition rate, R_d (refer to Table III, period 1 data) indicating the rate of suspended biomass deposition is limited by the rate of bacterial particle transport to the surface rather than the rate of cell adhesion at the surface.

The effect of changing fluid flow regime on eq. (12) is not so clear, for Beal[16] has indicated k_m to be a complex function of fluid velocity, fluid properties, particle size, and particle physical properties. Increasing fluid velocity can have the following two effects: 1) increased turbulence may increase or decrease the mass transfer coefficient k_m depending on the size of

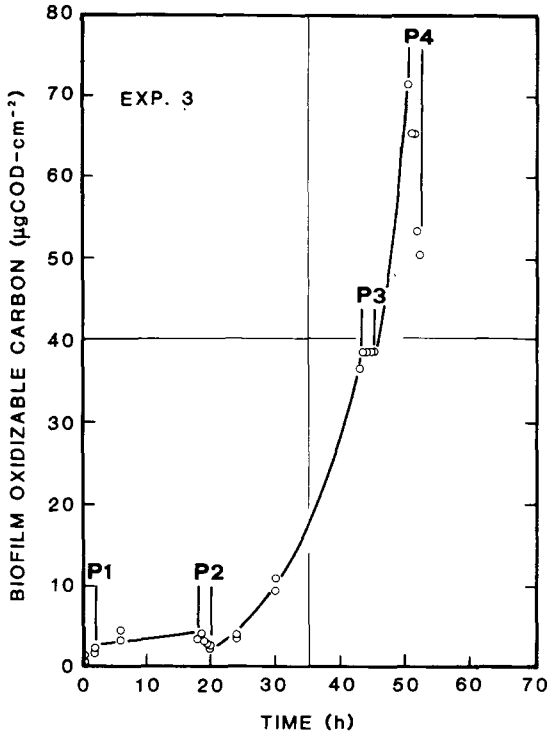

Fig. 11. Biofilm COD accumulation during experiment No. 3, where Re = 2.6×10^4 and X = 19.4 mg/L.

particle;[15,16] 2) increased turbulence may decrease the mass transfer boundary layer thus increasing transport to the surface.[30]

For the suspended biomass particles in these experiments (specific gravity = 1.05 and equivalent diameter = 3.0–5.0 μm), particle transport theory[16] predicts the mass transfer coefficient, k_m (and thus particle flux, N_x) to increase with increasing Reynolds number. However, Table III shows measured deposition rate, R_d is essentially unaffected by doubling Reynolds number (at Re = 1.3×10^4, R_d = 1.1 μg COD cm^{-2} h^{-1} while at Re = 2.6×10^4, R_d = 0.8 μg COD cm^{-2} h^{-1}). The discrepancy between Reynolds number effects on predicted particle transport flux and measured deposition rate arises because R_d encompasses both cell transport rate and cell adhesion rate. Therefore, while the predicted particle flux may increase with increasing Reynolds number, the overall deposition rate may not, which suggests that the rate of cell adhesion (or the cell "*sticking efficiency*") is decreasing with increasing Reynolds number. Duddridge, Kent, and Laws,[31] in adhesion studies with *Pseudomonas fluorescens*, also conclude that sticking efficiency decreases with increasing shear stresses.

Suspended biomass transport to and adhesion at a clean surface is a prerequisite to further biofilm formation. Results above suggest that the relative

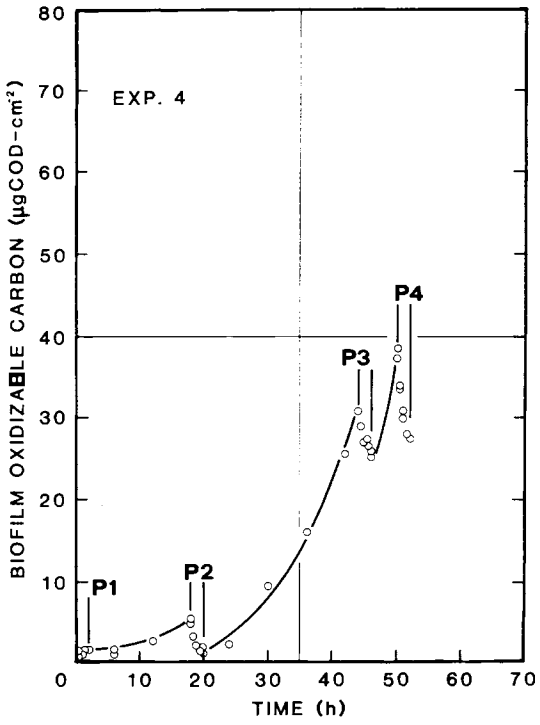

Fig. 12. Biofilm COD accumulation during experiment No. 4, where Re = 1.3×10^4 and $X = 4.0$ mg/L.

contribution of biomass deposition rate to the net accumulation rate of biofilm decreases with biofilm development. The reader is reminded, however, that the above conclusion is predetermined since R_d is assumed constant at the period 1 value of dB/dt. The authors feel that R_d should increase asymptotically with biofilm accumulation due to the *stickier* biofilm surface versus that of the clean tube. Unfortunately, the magnitude of this enhanced deposition was not measured in experiments presented here.

Biofilm Production

Values of μ_p are determined using eq. (7) and are given in Figure 15. In all experiments, μ_p decreases with increasing biofilm COD approaching the same asymptotic value of 0.1-0.2 h^{-1}, which is not surprising since effluent substrate concentrations from CSTR 2 are approximately the same in all four experiments. Wide variations in μ_p initially may result from inaccuracies in biofilm COD measurements at very low levels or changes in cellular metabolism upon initial adsorption. Decreases in μ_p with increasing biofilm COD could result from changes in cell metabolism or increasing internal substrate mass transfer resistance within the biofilm.

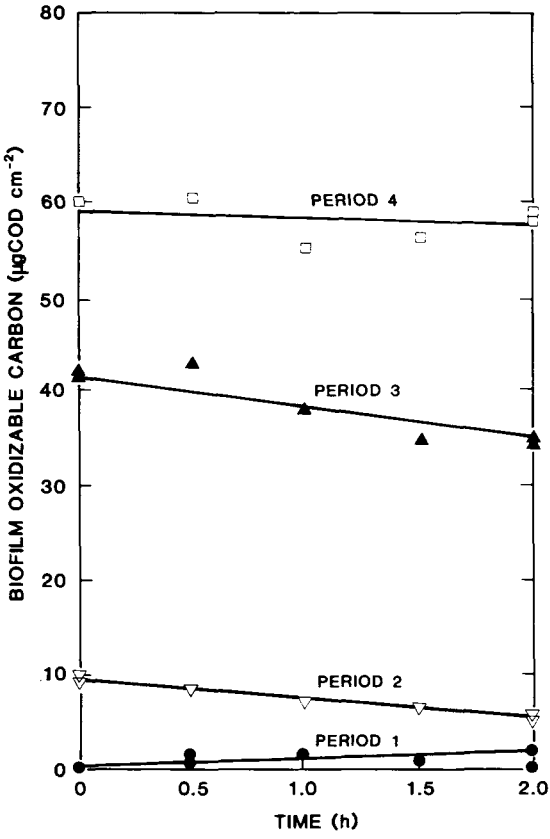

Fig. 13. Biofilm COD accumulation during four perturbation periods in experiment No. 2. Definition of conditions during each period is given in Fig. 8.

Instantaneous yield values in all experiments can be calculated from the substrate material balance, eq. (5), or upon rearrangement:

$$Y(t) = (\mu_p BA + \mu XV)/F(S_i - S) \tag{13}$$

Equation (13) tacitly assumes that yield coefficients for attached and suspended growth are the same. A summary of yield calculations is given in Table V and suggests an average yield of approximately 0.5 mg COD biomass/mg COD removed. This value compares favorably with those obtained by Stathopoulos[32] for similar experimental systems.

Although μ_p steadily decreases throughout early biofilm formation, results indicate the production rate of biofilm, $(\mu_p B)$, to be the largest positive contribution to net biofilm accumulation offset only by biofilm removal due to shear forces (see below).

TABLE III
Biofilm Accumulation during CSTR 2 Perturbations

	B[a] (μg COD/cm^2)	dB/dt[b] (μg COD cm^{-2} h^{-1})	k_eB (μg COD cm^{-2} h^{-1})
Experiment No. 1			
period 1	1.2	1.2	ND
2	ND	ND	ND
3	63.5	8.0	0.38
4	48.3	−5.3	ND
Experiment No. 2			
period 1	1.1	1.1	ND
2	7.3	−2.4	ND
3	38.8	−2.9	0.23
4	57.5	−2.5	ND
Experiment No. 3			
period 1	0.8	0.8	ND
2	2.5	−0.4	ND
3	38.5	0	0.22
4	61.0	−10.8	ND
Experiment No. 4			
period 1	0.3	0.3	ND
2	2.8	−2.2	ND
3	28.0	−3.0	0.17
4	33.0	−6.0	ND

[a]Average biofilm during perturbation;
[b]Accumulation during perturbation period only; ND = not determined.

Biofilm Decay

The specific biofilm decay rate is 0.006 h^{-1} which corresponds to values reported by Lawrence and McCarty[33] for suspended biomass (0.0019-0.22 h^{-1}) and Stathopoulos[32] for biofilm experiments at temperatures ranging from 15 to 45°C (0.04-0.22 h^{-1}). For the thin biofilms observed here, endogenous decay rates are considered a negligible influence on net biofilm accumulation. This may not be true in much thicker biofilms when transport of essential nutrients is reduced and microbial population densities are higher.

Biofilm Removal

Biofilm removal rates, R_r, over the range of biofilm COD observed (Fig. 14) reach maximum levels early in each experiment and these maximum values appear independent of either Reynolds number or suspended biomass concentration. Maximum biofilm removal rates in all experiments are less than 5 μg COD cm^{-2} h^{-1} except in period 4, experiment No. 3, where the R_r value increases from 1.0 μg COD cm^{-2} h^{-1} (at biofilm COD=45 μg

TABLE IV
Summary of Biofilm Removal Rate Calculations

	B (μg COD/cm^2)	dB/dt (μg COD cm^{-2} h^{-1})	R_d (μg COD cm^{-2} h^{-1})	$k_e B$ (μg COD cm^{-2} h^{-1})	R_r (μg COD cm^{-2} h^{-1})
			[a]	[b]	[c]
Experiment No. 1					
Period 1	1.8	+1.2	1.2	[d]	0
2	ND	ND	1.2	ND	ND
3	63.5	+8.0	1.2	0.4	−7.2
4	48.3	−5.3	[e]	0.3	5.0
Experiment No. 2					
Period 1	1.1	+1.1	1.1	[d]	0
2	7.3	−2.4	1.1	0.04	3.5
3	38.8	−2.9	1.1	0.2	3.8
4	57.5	−1.4	[e]	0.3	2.2
Experiment No. 3					
Period 1	0.8	0.8	0.8	[d]	0
2	2.5	−0.4	0.8	0.2	1.2
3	38.5	0	0.8	0.2	0.6
4	61.0	−10.8	[e]	0.4	10.4
Experiment No. 4					
Period 1	0.3	0.3	0.3	[d]	0
2	2.8	−2.2	0.3	0.02	2.5
3	28.0	−3.0	0.3	0.2	3.1
4	33.0	−6.0	[e]	0.2	5.8

[a]Deposition rate assumed constant at value of dB/dt determined in period 1; ND = not determined.
[b]Biofilm specific decay constant $k_e = 0.006$ h^{-1} for all experiments.
[c]Calculated from eqs. (9) or (10) (see Fig. 8).
[d]Assumed to be zero during period 1.
[e]Assumed zero during period 4.

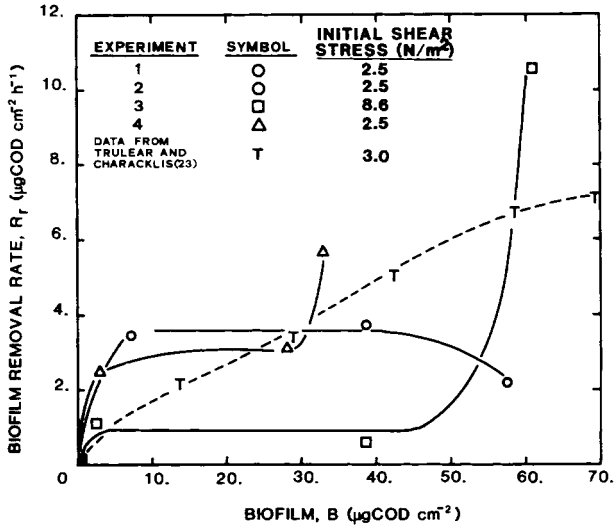

Fig. 14. Biofilm removal rate (R_r) estimates as a function of biofilm accumulation.

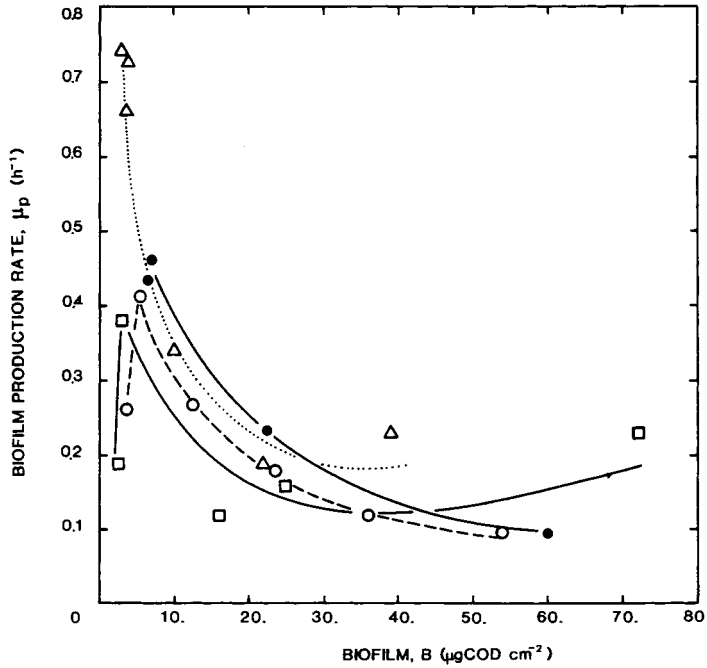

Fig. 15. Specific biofilm production rate (μ_p) estimates as a function of biofilm accumulation using eq. (7). Symbols: (○) experiment No. 1, (●) No. 2, (□) No. 3, (△) No. 4.

TABLE V
Summary of Calculations for Yield Coefficients

Time (h)	$F(S_i - S)$ (mg COD/h)	B (mg COD/cm^2)	μ_p[(1)] (h^{-1})	$\mu_p BA$ (mg COD/h)	X (mg COD/L)	$\mu X V$[b] (mg COD/h)	Y[c] (mg COD/mg COD)
Experiment No. 1							
0	52.7	0.001	0.70	0.5	18.7	29.3	0.57
10	79.6	0.005	0.40	11.8	24.0	37.6	0.62
34	150.6	0.019	0.20	22.5	28.9	45.3	0.45
50	149.6	0.035	0.13	27.0	26.5	41.5	0.46
Experiment No. 2							
0	0	0.001	0.10	0.5	18.9	29.6	— —
2	96.9	0.003	0.25	4.4	25.5	39.9	0.46
6	101.1	0.005	0.47	13.9	24.	37.6	0.51
20	103.4	0.007	0.45	18.7	22.5	35.3	0.52
46	208.4	0.030	0.18	32.0	25.0	39.2	0.34
Experiment No. 3							
6	81.6	0.005	0.35	10.4	22.7	34.6	0.55
18	81.6	0.005	0.35	10.4	22.7	34.6	0.55
24	84.0	0.006	0.32	11.6	22.1	34.6	0.55
30	96.2	0.011	0.25	16.3	22.0	34.5	0.53
50	106.4	0.055	0.16	52.2	22.5	35.3	0.42
Experiment No. 4							
6	14.3	0.001	0.75	4.5	3.0	4.7	0.64
20	31.4	0.002	0.70	8.3	4.2	6.6	0.47
44	110.5	0.020	0.24	28.5	12.0	18.8	0.43
50	106.8	0.035	0.24	49.8	12.0	18.8	0.64
51	89.9	0.033	0.24	46.9	7.0	11.0	0.64

[a]Biofilm production rate constants taken from Fig. 15 at specific biofilm COD.
[b]Suspended biomass growth rate, μ, with an assumed value of 0.33 h^{-1}.
[c]From eq. (13).

COD/cm^2) to 10.8 μg COD cm^{-2} h^{-1} (at biofilm COD=61.0 μg COD/cm^2). An explanation of this large difference in removal rate between these two points in biofilm accumulation can be given by considering the changes in hydrodynamic conditions that occur between the two levels of biofilm COD in question. The viscous sublayer thickness, δ, in a circular tube can be calculated from eq. (14):

$$\delta = 25d\,(\mathrm{R_e})^{-0.875} \tag{14}$$

Under the conditions of experiment No. 3 (pipe diameter, $d = 1.27 \times 10^4$ μm and Re $= 2.6 \times 10^4$) the viscous sublayer is ca. 44 μm. Biofilm levels of 45 and 61 μg COD/cm^2 correspond to biofilm thicknesses of 39.5 and 53.0 μm, respectively (with 1 mg biofilm = 1.74 mg biofilm COD and biofilm density = 10.0 mg biofilm cm^{-3}).[23,24] Comparison of the above calculations indicates the biofilm thickness, just prior to period 4 in experiment No. 3, exceeds the viscous sublayer thickness. Characklis[25] and co-workers[5,6] have shown that when a biofilm exceeds the viscous sublayer in a flow system, the frictional resistance increases dramatically. In a constant velocity system, as the frictional resistance increases, so must the shear stresses at the biofilm-fluid interface. An increase in shear stress could result in the dramatic increase in observed biofilm removal rate. Viscous sublayer thickness at Re $= 1.3 \times 10^4$ (experiment Nos. 1, 2, and 4) is 80 μm while biofilm thickness in the three experiments never exceeds ca. 66 μm. Thus, no radical increase in biofilm removal is expected and none are observed (see Fig. 14).

The magnitude of biofilm removal rates R_r can be checked independent of biofilm COD measurements, using the suspended biomass material balance applied to period 4 data. In period 4, suspended biomass from CSTR 1 is not supplied to CSTR 2. Therefore, after this 2-h period (eight CSTR 2 reactor residence times) any suspended biomass leaving the system must have originated from the biofilm. Consequently the rate of any suspended biomass leaving CSTR 2 after this perturbation can be considered equal to the rate of biofilm removal, i.e.,

$$R_r = FX/A \tag{15}$$

Table VI indicated the biofilm removal rates determined from biofilm COD [eq. (10)] are somewhat *less*, but of the same order, as values determined from the suspended biomass material balance, eq. (15).

Biofilm removal rates, for the aerobic, heterotrophic biofilms observed here, significantly influenced net biofilm accumulation. Results indicate biofilm removal rates, due to shear forces, is the only process to significantly detract from the biological production rate of biofilm. This may not be true in other fixed film processes—i.e., nitrifying biofilms—where equivalent levels of biofilm produce negligible suspended material[34] suggesting 1) removal rates are extremely low and 2) related to biofilm production rate.

TABLE VI
Comparison of Biofilm Removal Rate Estimates

Experiment No.	Re	CSTR 2 effluent biomass[a] (μg COD/L)	R_r [eq. (15)][b] (μg COD cm^{-2} h^{-1})	R_r [eq. (10)] (μg COD cm^{-2} h^{-1})
3	26000	5358	16.3	10.8
4	13000	1938	5.9	5.8

[a]Determined after eight residence times from start of period 4.
[b]Evaluated using $F = 18$ L/h and $A = 5934$ cm^2.

Limitations of Reported Results

Values of μ_p, k_e, Y, R_r, and R_d with increasing biofilm accumulation (B) are estimated during periods of perturbations in operating conditions of CSTR 2. Certain limitations may restrict the *general* usefulness of these results:

1) Biofilm accumulation was restricted to the early formation periods prior to any fluid frictional resistance increases. Consequently, results are restricted to aerobic biofilms with maximum thicknesses never exceeding 80 μm.

2) Analytical techniques required destructive sampling of the attached biomass which limited the number of samples taken during perturbations in CSTR 2 and influenced *precision* of dB/dt estimates.

3) Processes other than those considered may contribute to biofilm accumulation.

4) Results may be artifacts of the particular experimental method employed. The perturbations to CSTR 2 themselves may bias subsequent biofilm development; e.g., periods of substrate deprivation may influence the subsequent activity of the adherent microorganisms.

5) Reported values of biofilm removal rates, R_r are calculated from data obtained during system perturbations, i.e., at periods of "nongrowth" of biofilm. Subsequent calculations of biofilm specific production rate, μ_p, are based on the assumption that R_r values can be extrapolated to values of biofilm COD during unperturbed "growth" periods. If this assumption is valid, then during normal operating conditions the suspended biomass material balance, eq. (6), and the biofilm accumulation equation, eq. (7), can be equated, i.e.,

$$dB/dt - (\mu_p - k_e)\, B = [F(X_i - X) + \mu XV]/A \qquad (16)$$

Equation (16) can be evaluated at different times throughout an experiment using values of μ_p given in Figure 15. Results, given in Table VII, indicate *poor agreement* between the biofilm portion (left-hand side) and the suspended biomass portion (right-hand side) of eq. (16). This discrepancy is, in part, due to inaccuracies in suspended biomass determinations. However, these inequalities may also indicate that values of R_d, R_r, and μ_p determined

TABLE VII
Evaluation of eqs. (6) and (7); Extrapolation Validity of Perturbation Results

Experiment No.	Elapsed time (h)	dB/dt (μg COD cm^{-2} h^{-1})	μ_p[a] (h^{-1})	μXV[b] (μg COD/h)	$dB/dt - (\mu_p - k_e)B$ (μg COD cm^{-2} h^{-1})	$[F(X_i - X) + \mu XV]/A$ (μg COD cm^{-2} h^{-1})
1	0	1.2	0.10	29500	1.1	5.0
	10	0.2	0.40	37900	−1.2	5.1
	34	18.0	0.20	45700	14.3	4.5
	50	36.0	0.13	41900	31.7	4.2
2	0	0.3	0.10	29900	0.2	4.2
	2	0.3	0.25	40300	−0.4	5.2
	6	0.7	0.47	37900	−2.8	6.7
	20	0.9	0.45	35600	−2.2	2.8
	46	2.5	0.18	39500	−2.7	3.4
3	6	0.15	0.35	34960	−0.50	10.1
	18	0.80	0.35	34960	−0.40	9.2
	24	1.0	0.33	34960	−0.30	22.7
	30	7.5	0.25	34800	−0.45	12.3
	50	16.0	0.16	35600	+4.90	9.9
4	6	0.05	0.75	4240	0.7	0.33
	20	0.05	0.70	6640	1.3	0.45
	44	1.80	0.24	18980	−2.9	−3.20
	50	3.3	0.24	18980	−4.9	−6.50
	51	3.3	0.24	11100	−4.4	−7.40

[a]Biofilm growth rate at specific biofilm COD; taken from Fig. 15.
[b]Suspended biofilm growth rate, μ, assumed equal to the dilution rate of CSTR 1, $= 0.33$ h^{-1}.

from perturbation data, are artifacts of the unsteady-state method and cannot be extrapolated to steady-state conditions. For example, the biofilm portion of eq. (16) may be too low due to high values of μ_p brought about by underestimating either R_d or R_r. Deposition rate, R_d, is assumed constant in all calculations at the period 1 estimate of dB/dt, which ignores increases in deposition rate brought about by the sticky biofilm surface. Therefore, R_d values reported mostly likely underestimated deposition rates late in each experiment. The suspended biomass portion of eq. (16) may be too high due to overestimating the suspended biomass production rate, μXV, brought about by inaccuracies in suspended biomass measurements or by overestimating μ (see point 6 below).

6) Specific growth rate of suspended organisms in CSTR 1 may not represent the specific growth rate of suspended organisms in CSTR 2 since the organisms have been subjected to a significant change in growth environment.

CONCLUSIONS

This article has described processes contributing to the net rate of primary biofilm accumulation in a tubulent flow system. Results are restricted to thin aerobic biofilm in their early stages of formation.

Conclusions drawn from this work and subject to limitations stated above include the following:

Deposition

Suspended biomass deposition is a prequisite to biofilm formation but the relative contribution of biomass deposition to biofilm net accumulation decreases with biofilm development.

Suspended biomass deposition rate is directly proportional to suspended biomass concentration which suggests deposition in these experiments is controlled by particle transport to the surface rather than cellular adhesion.

Deposition rates are unaffected by doubling the Reynolds number. Particle transport theory[16] predicts an increase in particle flux with increasing Reynolds number. Since deposition rate is the sum of both particle transport and cellular adhesion rates, results imply cell adhesion (or cell "sticking efficiency") decreases with increasing Reynolds number.

Decay

The biofilm decay rate, for the thin biofilms observed, is a negligible influence on net biofilm accumulation.

Production

Biofilm production, due to microbial cell reproduction and extracellular-polymer production, is the major positive contribution to biofilm net accumulation.

Although CSTR 2 is operated at a dilution rate sufficiently greater than washout, suspended biomass growth and concomittant substrate utilization are significant.

Estimates of stoichiometry (i.e., yield coefficients) in biofilm reactors must account for the total biomass produced. Traditional definitions of yield for CSTRs, based on effluent substrate and biomass concentrations alone, neglect biofilm mass and thus underestimate true stoichiometric yield.

Removal

Biofilm removal rate is the only process that significantly offsets the biological production of biofilm, thus detracting from biofilm net accumulation.

Biofilm removal, due to shear forces, occurs continually throughout biofilm development and increases dramatically if the biofilm exceeds the existing viscous sublayer.

This work was done at the Department of Environmental Science and Engineering, Rice University, Houston, Texas with financial support from the National Science Foundation (77-26934), Electric Power Research Institute (RP902-1), and the Amoco Foundation Environmental Research Fellowship. The authors express their gratitutde to Dr. Michael G. Trulear and Dr. Willi Gujer for their thorough and helpful review of the manuscript. Preparation of the manuscript by Frieda Schlumpf was supported by EAWAG.

References

1. K. C. Marshall, *Interfaces in Microbial Ecology* (Harvard University Press, Cambridge, MA, 1976).

2. G. Bitton and K. C. Marshall, Eds., *Adsorption of Microorganisms to Surfaces* (Wiley, New York, 1980).

3. J. W. Costerton and G. G. Geesey, "Which population of aquatic bacteria should we enumerate?" *Native Aquatic Bacteria: Enumeration, Activity, and Ecology*, ASTM-STP No. 695, J. W. Costerton and R. R. Colwell, Eds. (Am. Soc. Testing Mater., Philadelphia, PA, 1979).

4. W. G. Characklis, *Water Res.*, **7**, 1249 (1973).

5. N. Zelver, "Biofilm development and associated energy losses in water conduits," M. S. thesis, Rice University, Houston, TX, 1979.

6. B. F. Picologlou, N. Zelver, and W. G. Characklis, *J. Hydraulic Div., ASCE*, **106** (1979).

7. A. H. Booth, *J. Appl. Bacteriol.* **27**, 174 (1964).

8. J. D. A. Miller and R. A. King, "Biodeterioration of metals," *Microbial Aspects of the Deterioration of Materials*, R. J. Gilbert and D. W. Lovelock, Eds. (Academic, New York, 1975).

9. R. B. Ritter, J. W. Suitor, and G. A. Cypher, "Thermal fouling rates of 90-10 Cu-Ni and Ti in seawater service," report to Int. Copper Res. Assoc., Inc. by Heat Transfer Research, Inc., Alhambra, CA, 1977.

10. M. J. Nimmons, "Heat transfer effects in turbulent flow due to biofilm development," M. S. thesis, Rice University, Houston, TX, 1979.

11. R. E. Baier, "Influence of the initial surface condition of materials on bioadhesion," *Proc. 3rd Int. Congr. Mar. Corr & Fouling* (Natl. Bureau of Standards, Gaithersburg, MD, 1972).

12. R. E. Baier, *Applied Chemistry at Protein Interfaces*, Division of Colloid and Surface Science, 166th Adv. Chem. Ser. 145, R. E. Baier, Ed. (Am. Chem. Soc., New York, 1973).

13. G. I. Loeb, and R. A. Neihof, "Molecular fouling of surfaces in seawater," *Proc. 3rd Int. Cong. Mar. Corr. and Fouling* (National Bureau of Standards, Gaithersburg, MD, 1972).

14. G. I. Loeb and R. A. Neihof, "Marine conditioning films," *Applied Chemistry at Protein Interfaces.* Adv. Chem. Ser. 145, R. E. Baier, Ed. (Am. Chem. Soc., New York, 1973).

15. S. K. Friedlander and H. F. Johnstone, *Ind. Eng. Chem.*, **49,** 1151 (1957).

16. S. K. Beal, *Nucl. Sci. Eng.*, **40** (1970).

17. D. H. Lister, "Corrosion products in power generating systems," *Proc. Int. Conf. Fouling Heat Trans. Equip.* (Rensselaer Polytechnic Institute, Troy, NY, 1979).

18. W. A. Corpe, "Attachment of marine bacteria to solid surfaces," *Adhesion in Biological Systems,* R. S. Manly, Ed. (Academic, New York, 1970).

19. M. Fletcher and G. D. Floodgate, *J. Gen. Microbiol.* **74,** 325 (1973).

20. M. Fletcher, *J. Gen. Microbiol.* **94,** 400 (1976).

21. M. Fletcher, *Can. J. Microbiol.*, **23,** 1 (1977).

22. K. C. Marshall, R. Stout, and R. Mitchell, *J. Gen. Microbiol.*, **68,** 337 (1971).

23. M. G. Trulear and W. G. Characklis, "Dynamics of biofilm processes," *Proc. 34th Ann. Purdue Inc. Waste Conf.* (Purdue University, West Lafayette, IN, 1979).

24. J. D. Bryers, "Dynamics of early biofilm formation in a turbulent flow system," Ph.D. thesis, Rice University, Houston, TX, 1980.

25. W. G. Characklis, *Biotechnol. Bioeng.*, **23,** 1923 (1981).

26. J. D. Bryers and W. G. Characklis, "Kinetics of initial biofilm formation within a turbulent flow system," *Proc. Int. Conf. Fouling of Heat Transf. Equip.* (Rensselaer Polytechnic Institute, Troy, NY, 1979).

27. J. D. Bryers and W. G. Characklis, *Water. Res.*, **15,** 483 (1981).

28. *Standard Methods for The Examination of Water and Wastewater, 14th ed.* (American Public Health Assoc, Washington, DC, 1977).

29. L. W. B. Browne, *Atm. Environ.* **8,** 801 (1974).

30. R. B. Bird, W. E. Stewart, and E. N. Lightfoot, *Transport Phenomena* (Wiley, New York, 1960).

31. J. E. Duddridge, C. A. Kent, and J. F. Laws, *Biotechnol. Bioeng.*, **24,** 153 (1982).

32. N. Stathopoulos, M. S. thesis, Rice University, Houston, TX, 1980.

33. A. W. Lawrence and P. L. McCarty, *J. Sanit. Eng. Div., ASCE,* **96,** SA3 (1970).

34. J. Bryers, unpublished results, EAWAG, Dübendorf, Switzerland, 1982.

Accepted for Publication May 18, 1982